K. A. Ellison, J. A. Daleo and D. H. Boone

BWD Turbines Ltd. 1-601 Tradewind Dr., Ancaster, Ontario L9G 4V5

Abstract

Interdiffusion between a NiCoCrAlYRe coating and an IN-738 blade alloy substrate was investigated. Tests were conducted by exposing coated blade specimens in still air at 940°C and 1050°C for times of up to 9720 h. The interdiffusion zone microstructures were characterized by scanning electron microscopy and energy dispersive x-ray spectroscopy. It was found that at 1050°, the central NiCoCrAlYRe coating was comprised of γ , β and α phases and that a continuous α -Cr layer formed along the original substrate interface. At 940°C a more complex sequence of interdiffusion microstructures was observed, including the formation of a continuous $\gamma' + \alpha$ zone adjacent to the blade alloy substrate. The NiCoCrAlYRe coating was also comprised of four phases at the lower exposure temperature: γ , β , α and σ . It is shown that the complex interdiffusion behavior requires the use of diffusion path analysis for proper interpretation. The implications for development of service temperature estimation models based on coating/substrate interdiffusion in this system are discussed.

Introduction

Overlay coatings of the NiCoCrAlY type are used extensively for protection of hot section components in gas turbine engines. Commercial NiCoCrAlY coatings are based on the $\gamma\text{-FCC}$ and $\beta\text{-(Ni,Co)Al}$ phases, but they may in addition contain phases such as γ' , $\alpha\text{-Cr}$ and $\sigma\text{-(Cr}_x\text{Co}_y)$. 2,3 Rhenium alloying is reported to improve the oxidation resistance and stability of NiCoCrAlY coatings. The nickel-based superalloys used for rotating blades are primarily comprised of the γ and $\gamma'\text{-(Ni}_3\text{Al)}$ phases. Interdiffusion between the coatings and substrates results in complex microstructural transformations which vary with the alloy compositions, temperature and time. 4

of interdiffusion between the rates Co-29Cr-6.5Al-0.5Y (wt %) coating and a nickel-base superalloy substrate were quantified and used to predict the service operating temperatures of a combustion turbine blade airfoil.5 metallurgical temperature estimates are used to calibrate finite element heat transfer models that support turbine hot section component life and repair calculations in an integrated approach to life management. 6,7,8 It would be quite useful if this type of temperature estimation model could be extended more generally to other commercial coating / substrate systems. However, a qualitative description and understanding of the diffusional interactions and microstructural transformations that occur at turbine operating temperatures is required before this can be accomplished. In this investigation, the interdiffusion behavior in NiCoCrAlYRe-coated IN-738 was evaluated at 940° and 1050°C.

Experimental Procedures

The chemical compositions of the IN-738LC blade and NiCoCrAlYRe coating alloys used in this investigation are given in Tables I and II. The commercial name for the NiCoCrAlYRe coating is SICOAT 2453.* The sample material was sectioned from commercially processed gas turbine blades. The as-received coating was approximately 200 µm thick. After transferred are cleaning and deposition by low pressure plasma spray (LPPS), the coating was diffusion bonded to the alloy substrates by annealing in vacuum at 1120°C for 2-4 hours. The coated blade was then aged at 843°C for 24 hours.

Table I Nominal composition of IN-738LC (weight percent).

Ni	Со	Cr	Al	Ti	Мо	W	Ta	Nb	Zr	В	С
Bal.	8.5	16.0	3.4	3.4	1.75	2.6	1.75	0.85	0.12	0.012	0.13

Table II Chemical composition of NiCoCrAlYRe coating (weight percent).

Ni	Со	Cr	A1	Re	Y
Bal.	8.8	24.4	10.7	2.3	0.5

The coating samples were isothermally exposed in still air for up to 9,720 hours at 940° and 1050°C. The samples were removed from the furnaces and rapidly quenched in air to preserve the high temperature microstructures. The coating interdiffusion zones were examined by optical and scanning electron microscopy. The microstructural features were revealed by backscattered electron (BSE) imaging and after etching in a 1% chromic acid solution at 5VDC. The various phases in the coatings were identified on the basis of energy dispersive spectroscopy (EDS) results obtained from unetched specimens using a LINK Analytical QX2000 analyzer attached to a Phillips 515 scanning electron microscope operated at 20 keV.

649

^{*} SICOAT 2453 is a designation of Siemens AG, Power Generation (KWU), Mülheim, Germany

Results

Interdiffusion at 1050°C

A coating sample exposed for 1300 h at 1050°C is shown in Figure 1. Compared with CoCrAlY / Ni-base and CoNiCrAlY / Ni-base samples studied previously^{5,9}, the coating was relatively intact and retained a substantial amount of beta phase within the central coating layer. Large Kirkendall-type pores were observed along the substrate interface.

A magnified view of the coating/substrate interdiffusion zone is shown in Figure 2. The central coating region was comprised of three principal phases: the γ matrix, β -(NiCo)Al and Cr,Re-rich α precipitates, Table III. Most of the rhenium partitioned to the α phase, which appeared white in BSE imaging mode. Interdiffusion between the NiCoCrAlYRe coating and IN-738 alloy resulted in the formation of a β -depletion zone above the original substrate interface leaving only the γ and α phases. Along the original interface, the α precipitates formed an essentially continuous layer. This zone was followed by a single-phase γ zone immediately adjacent to the γ + γ' IN-738 alloy.

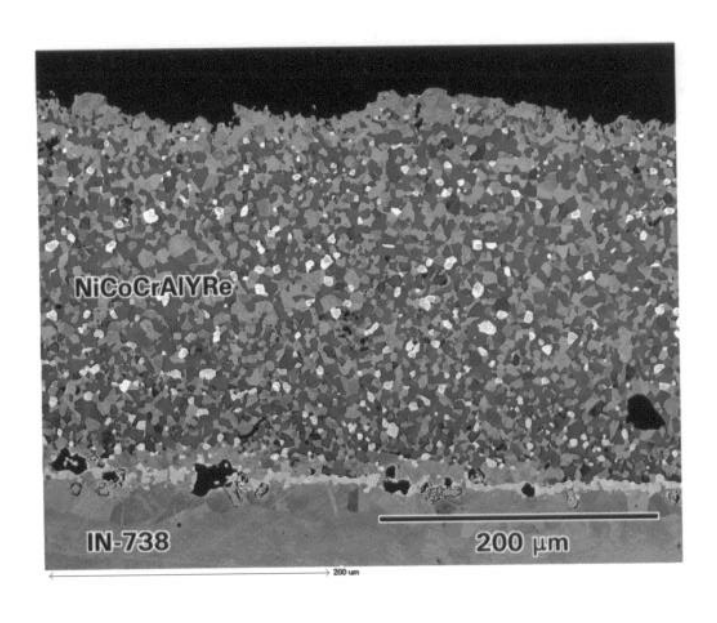


Figure 1: NiCoCrAlYRe coating after 1300 h at 1050°C (BSE image, unetched).

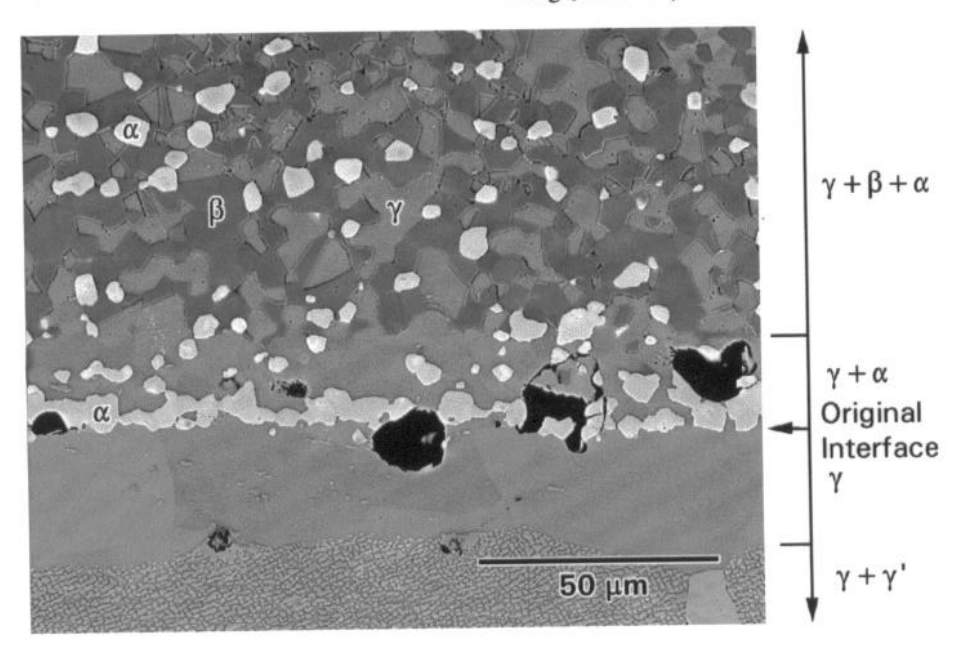


Figure 2: Interdiffusion zone microstructure after exposure for 1300 h at 1050°C (BSE image, 1% chromic).

Table III EDS results for individual phases identified in Figure 2 (atomic percent).

Ni	Co	Cr	Al	Ti	Ta	Mo	Re	Zone	Phase I.D.
15	5	8.5	40	1				$\gamma + \beta + \alpha$	β
45 43	11	32	13					$\gamma + \beta + \alpha$ $\gamma + \beta + \alpha$	γ
3.5	1.5	90	3.5				1	$\gamma + \beta + \alpha$	α
3.3	1.5	90	4			0.5	0.5	$\gamma + \alpha$	α
42.5	10.5	31.5	13.5	1		0.5		γ	γ

Interdiffusion at 940°C

The NiCoCrAlYRe coating exposed for 9,720 h at 940°C is shown in Figure 3. Once again, the coating was relatively undepleted after this length of exposure, compared to CoCrAlY / Ni-base and CoNiCrAlY / Ni-base samples examined in previous investigations. A magnified image of the coating / substrate interdiffusion zone is shown in Figure 4. At this temperature, the central coating zone was comprised of four phases: the γ matrix, β -(NiCo)Al, Cr-rich α and σ precipitates, Table IV. The rhenium partitioned to the α and σ phases, which each contained about 1 at % of this element. There was very little contrast difference between the two in BSE imaging mode.

The diffusion zone between the NiCoCrAlYRe coating and IN-738 substrate was more complex at 940°C as compared to that observed at 1050°C. Moving from the central coating zone towards the alloy substrate, the EDS results showed that the α precipitates disappeared, leaving a three-phase, $\gamma+\beta+\sigma$ zone. This was followed by a zone in which the β and σ precipitates also disappeared and were replaced by γ' and α (white in BSE mode). The three-phase $\gamma+\gamma'+\alpha$ zone extended down to the original coating/substrate interface. Below the original interface, a two-phase $\gamma'+\alpha$ structure was observed. In this zone the α phase precipitates were dark in BSE imaging mode and EDS analysis showed that that they contained almost no rhenium. The interface between the two-phase $\gamma'+\alpha$ zone and the $\gamma+\gamma'$ substrate was non-planar.

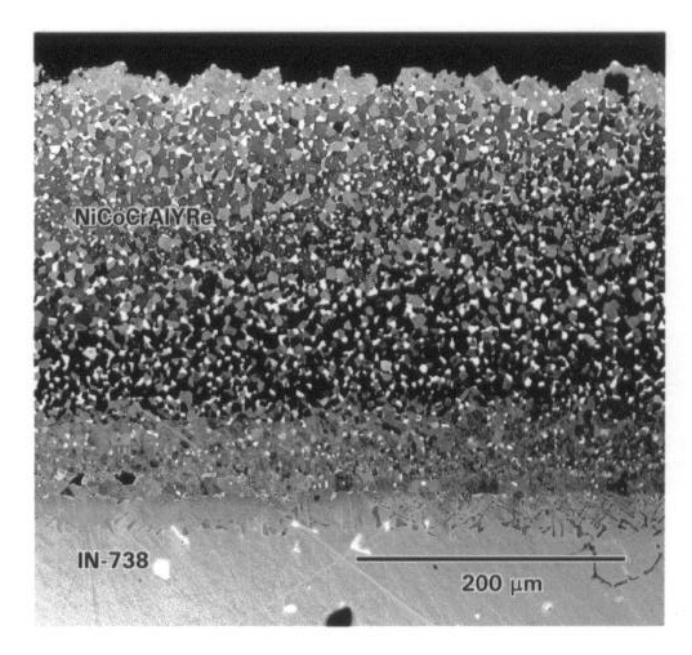


Figure 3: NiCoCrAlYRe coating after 9720 h at 940°C (BSE image, unetched).

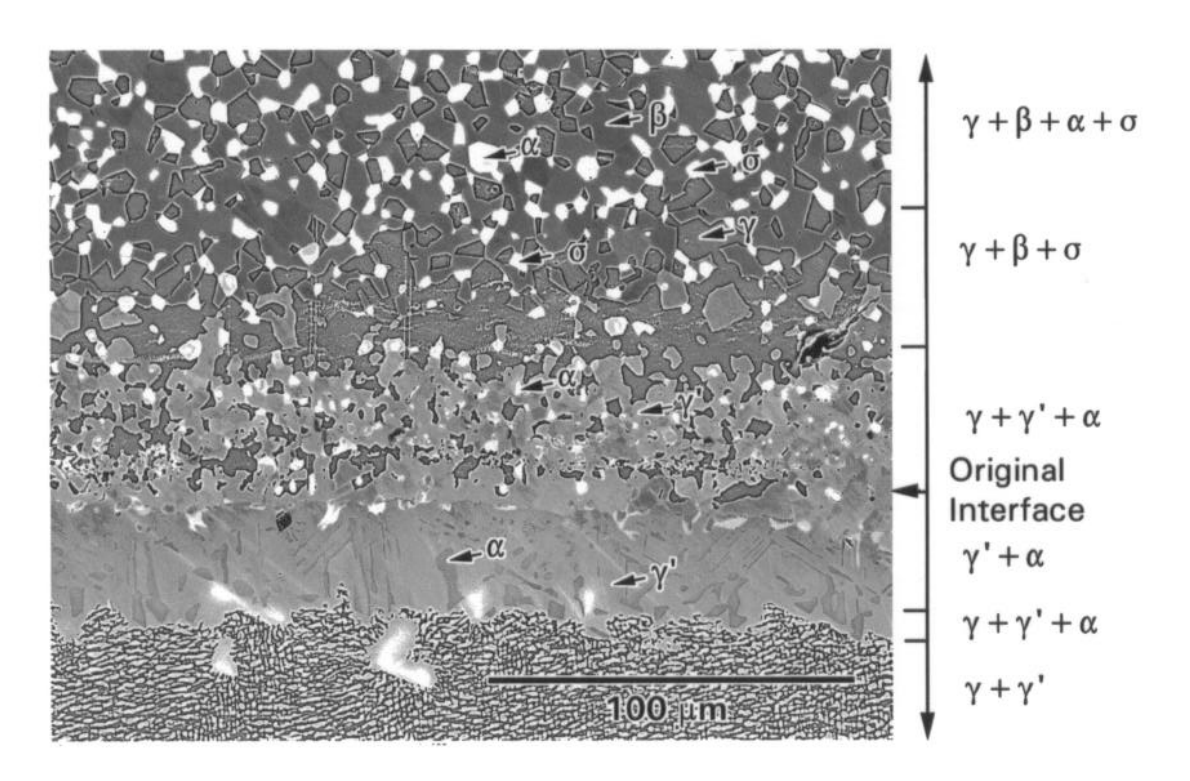


Figure 4: Interdiffusion zone microstructure after exposure for 9720 h at 940°C (BSE image, 1% chromic).

Ni	Со	Cr	Al	Ti	Та	Мо	Re	Zone	Phase I.D.
50	5	8	37					γ+β+α+σ	β
40	12.5	36	11					γ+β+α+σ	·γ
3.5	1.5	92	2				1	γ+β+α+σ	ά
12.5	12.5	70	3.5				1	$\gamma + \beta + \alpha + \sigma$	σ
58	6.5	10.5	23	2				$\gamma + \gamma' + \alpha$	ν'
4.5	2	89.5	2.5				1.5	$\dot{\gamma} + \dot{\gamma}' + \alpha$	ά
62	5.5	5	22	5			0.5	$\gamma' + \alpha$	ν'
7.5	2	85	1.5	0.5		2.5		$\gamma' + \alpha$	ά

Discussion

Interpretation of the Interdiffusion Zone Microstructures

The multi-phase diffusion zones at the coating / substrate interfaces can be represented in a compact way and related to the governing phase equilibria by plotting diffusion paths on the appropriate phase diagrams. A schematic isothermal phase diagram for Ni-Cr-Al at 1050°C is shown in Figure 5. This diagram is hypothetical but is based on the closest available Ni-Cr-Al^{11,12} section at 1025°C. A schematic diffusion path has been drawn to represent the NiCoCrAlYRe / IN-738 system after 1300 h at 1050°C. The multi-component NiCoCrAlYRe coating alloy was approximated as a Ni-Cr-Al ternary alloy by treating the chromium concentration of the α and σ phases as an equivalent (Crea = Cr + Re). This is a reasonable approximation since the rhenium tends to partition strongly with the chromium in the α and σ phases. ^2,3 Likewise, an equivalent aluminum concentration was used for the IN-738 (Alea = Al + Ti + Ta + Nb) since these elements tend to partition to and stabilize the γ' phase in $\gamma + \gamma'$ alloys. 13 Note that, the presence of minor phase constituents (e.g. MC, M23C6, Ni5Y and Y₂O₃) which are present in the commercial coating and substrate alloys cannot be represented within the Ni-Cr-Al ternary diagram.

The diffusion path of Figure 5 proceeds from the outer coating interface (point 1) to the IN-738 substrate (point 4). Oxidation at the outer coating surface of the NiCoCrAlYRe coating resulted in depletion of the α and β phases, so the initial part of the diffusion path is represented as residing closer to the y, single phase field (point 1). The path then moves upward as it passes through the central coating region, representing the higher aluminum concentrations and higher volume fractions of β phase within the "bulk" coating layer (point 2). Moving in the direction of the coating / substrate interface, the path drops down into the twophase $\gamma + \alpha$ phase field created by the depletion of aluminum from the coating into the alloy substrate. Enrichment of the a phase along the coating/substrate interface is represented by the loop towards the a single-phase field on the left of the diagram (point 3). The path then crosses back through the $\gamma + \alpha$ field. Since no distinct $\gamma + \alpha$ region was visible below the α particles. this portion of the diffusion path would lie on or close to a tie line through the $\gamma + \alpha$ field. The diffusion path then enters the γ

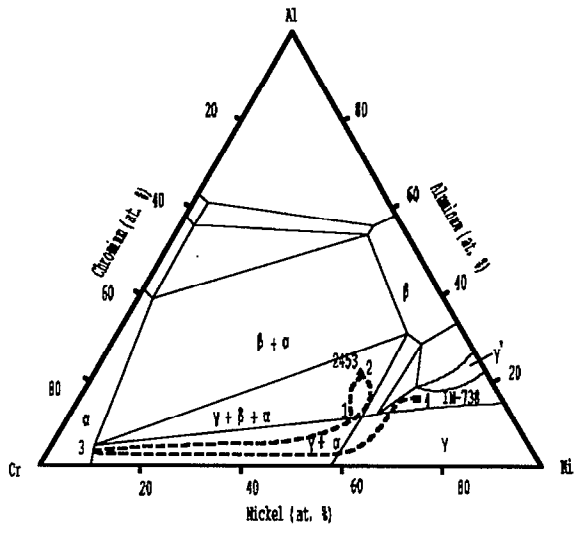


Figure 5: Schematic diffusion path (dashed line) for 1050°C interdiffusion between the NiCoCrAlYRe coating and IN-738 alloy substrate.

single-phase field before rising upwards into the $\gamma + \gamma'$ field and terminating at the equivalent IN-738 alloy composition (point 4).

The microstructural features produced by 940°C interdiffusion between the NiCoCrAlYRe coating and the IN-738 alloy substrate were more complex than at 1050°C and could not be represented on a single ternary phase diagram. According to the Gibbs phase rule, the four-phase $\gamma + \beta + \alpha + \sigma$ equilibrium observed in the central coating zone cannot be represented on anything less than a quaternary diagram. However, Sims¹⁴ has noted that, "... no observation of a 'quaternary' phase between metals has been reported thus, regardless of the number of (alloying) elements involved, all phase relations applying to any nickel- or cobalt-base superalloy can be expressed in terms no more complicated than quaternary diagrams."

Inspection of the available ternary diagrams shows that the Ni-Co-Cr-Al quaternary system contains all of the major phase constituents (e.g. γ , γ' , β , α and σ) observed in the present study. Until recently, no quaternary diagrams had been published in the Ni-Co-Cr-Al system.⁹ Too few data are available to permit speculation on the appearance of the interior regions of the

Ni-Co-Cr-Al diagram at 940°C. However, the faces of the pyramidal Ni-Co-Cr-Al quaternary diagram at 940°C can be represented to a first approximation by using the closest available Ni-Cr-Al^{11,12}, Ni-Co-Cr¹⁵, Co-Cr-Al^{16,17} and Ni-Co-Al¹⁸ ternary diagrams. Note that, the Ni-Cr-Al diagram at 850°C was used since there is an invariant transformation $(\gamma + \beta \leftrightarrow \gamma' + \alpha)$ at approximately 990°C. Using these diagrams, the pyramidal Ni-Co-Cr-Al section has been unfolded into a planar view, as shown in Figure 6. The Ni-Co-Al ternary section is not shown in Figure 6 since it is not critical to the explanation.

Diffusion paths that go through the interior of the quaternary pyramid cannot be mapped onto the unfolded Ni-Co-Cr-Al diagram. However, to a first approximation, the sequence of major phase fields observed between the bulk NiCoCrAlYRe coating and the IN-738 substrate traversed the Ni-Co-Cr-Al diagram close to the ternary faces. This is shown by the schematic diffusion path superimposed on Figure 6. The path originates at a point within the Ni-Cr-Al diagram representing the equivalent IN-738 composition (point 1). Moving towards the coating, the path climbs to higher aluminum concentrations and passes through the $\gamma + \gamma' + \alpha$ and $\gamma' + \alpha$ phase fields before reaching the original coating/substrate interface. It then crosses back through the $\gamma + \gamma' + \alpha$ field, identified above the coating/substrate interface. Next, the path crosses the $\gamma + \alpha$, $\gamma + \alpha + \sigma$ and $\gamma + \sigma$ phase fields, before entering the $\gamma + \sigma + \beta$ field on the Co-Cr-Al side of the diagram (point 2). Note that, the $\gamma + \alpha$, $\gamma + \alpha + \sigma$ and $\gamma + \sigma$ zones were not distinct in the diffusion zone microstructure, but a transition region between the $\gamma + \gamma' + \alpha$ and $\gamma + \sigma + \beta$ zones was apparent, as noted above. From the $\gamma + \sigma + \beta$ field, the path leading to the bulk coating composition would need to turn towards the interior region of the diagram, containing an adjacent $\gamma + \sigma + \beta + \alpha$ four-phase field. As noted earlier, this final segment of the path cannot be shown on the unfolded diagram.

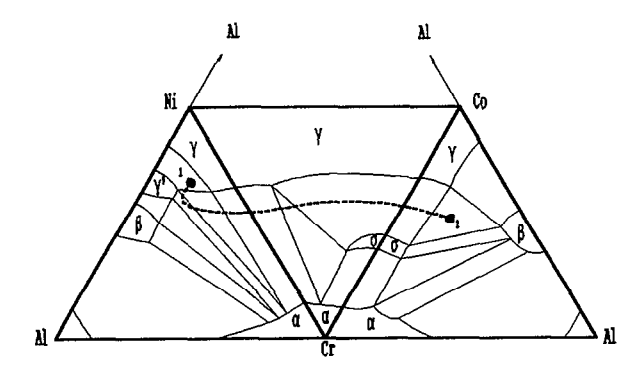


Figure 6: Schematic diffusion path (dashed line) for 940°C interdiffusion between the NiCoCrAlYRe coating and IN-738 alloy substrate.

Implications for Temperature Estimation

As described in Ref 5, the temperature estimation model for service-exposed CoCrAlY (GT-29) coatings on Ni-based (GTD-111) substrates was based on the rate of growth of the well-defined $\gamma + \beta$ zone below the original interface. This general feature of the interdiffusion zone was present over the temperature range of interest to the analysis of service-exposed turbine blades and growing at a rate sufficient to allow temperature estimates to be made with reasonable accuracy. A review of the Ni-Co-Al ternary system confirms that the $\gamma + \beta$ phase field is, in fact, stable over a very wide temperature range (150°C to 1300°C), although the extent of the two-phase region varies considerably with temperature. The latter effect was accounted for in the temperature estimation model by incorporating a constitutional term within the total activation energy for $\gamma + \beta$ zone growth.

Over the range of temperatures used in this investigation, significant constitutional changes occurred within the NiCoCrAlYRe coating and throughout the coating/substrate interdiffusion zone. These microstructural transformations prevent the calibration of a temperature estimation model based on growth of a single zone over a comparable range of temperatures. The rates of intermediate zone growth $(\gamma, \gamma' + \alpha)$ were also qualitatively slower in the NiCoCrAlYRe / Ni-base system than for $\gamma + \beta$ growth observed in the CoCrAlY / Ni-base and CoNiCrAlY / Ni-base systems examined previously. 5,9 The latter effect may be partly related to the formation of continuous α (at 1000°C and 1050°C) and $\gamma' + \alpha$ (at 940°C) zones between the NiCoCrAlYRe coating and IN-738 substrate. The transport of coating and substrate elements across these layers is expected to be slower than through intermediate layers comprised of a y matrix phase, as observed in the CoCrAlY / Ni-base and CoNiCrAlY / Ni-base systems. The reduced rates of intermediate zone growth in the NiCoCrAlYRe / Ni-base system would lead to greater uncertainty in temperature estimates based on this phenomenon.

As an alternative to layer growth, it might be possible to make use of constitutional changes within the coating and coating/substrate interdiffusion zones to establish benchmark temperature estimates for service exposed turbine components. For example, a change from γ to $\gamma' + \alpha$ formation was observed between 940°C and 1000°C below the original NiCoCrAlYRe/IN-738 interface. The diffusion path analysis showed that this was consistent with the presence of an invariant $\gamma + \beta \leftrightarrow \gamma' + \alpha$ transformation in the Ni-Cr-Al system at approximately 990°C. Additional transformations may occur within the coating and/or interdiffusion zones at lower temperatures. Further investigations are planned to explore this possibility in greater detail.

Conclusions

The interdiffusion behavior in the NiCoCrAlYRe-coated IN-738 system is complex and requires the use of diffusion paths for proper interpretation. Constitutional differences were observed both within the coating and coating/substrate interdiffusion zone at the two temperatures used in this investigation. The observed constitutional changes will make it necessary to develop alternative approaches for metallurgical temperature estimation based on coating/substrate interdiffusion.

Acknowledgements

Financial support for this work was provided, in part, by the National Research Council of Canada, Industrial Research Assistance Program.

References

- ¹ Proceedings of the Conference on "Protective Coating Systems for High-Temperature Gas Turbine Components", <u>Materials Science and Technology</u>, 2 (1986), 193-326.
- ² W. Beele, et al., "Long-term Oxidation Tests on a Re-containing MCrAlY Coating", <u>Surface and Coatings Technology</u>, 94-95 (1997), 41-45.
- ³ N. Czech, F. Schmitz and W. Stamm, "Microstructural Analysis of the Role of Rhenium in Advanced MCrAlY Coatings", <u>Surface and Coatings Technology</u>, 76-77 (1995), 28-33.
- ⁴ P. Mazars, D. Manesse, and C. Lopvet, "Degradation of MCrAlY Coatings by Interdiffusion" (Paper No. 87-GT-58, presented at the ASME/IGTI Gas Turbine Conference and Exhibition, Anaheim, California, May 31 June 4, 1987).
- ⁵ K. A. Ellison, J. A. Daleo and D. H. Boone, "Metallurgical Temperature Estimates Based on Interdiffusion Between CoCrAlY Overlay Coatings and a Directionally Solidified Nickel-Base Superalloy Substrate", <u>Materials for Advanced Power Engineering 1998</u>, ed. J. Lecomte-Beckers et al. (Jülich, Germany: Forschungszentrum Jülich GmbH Central Library, 1998), 1523 1534.
- ⁶ Daleo J.A., Boone D.H., "Metallurgical Evaluation Techniques In Gas Turbine Failure Analysis And Life Assessment", <u>Failures</u> 96, <u>Risk</u>, <u>Economy and Safety</u>, <u>Failure Minimization and Analysis</u>, ed R.K Penny (Rotterdam: Balkema, 1996, ISBN 9054108231), 187-201.
- ⁷ Woodford D. A., Daleo J.A., "Stress Relaxation as a Basis For Blade Creep Life Assessment" (Paper presented at the IOM conference "Life Assessment of Hot Section Gas Turbine Components", James Watt Centre, Heriot Watt University, Edinburgh, UK, Oct. 5 7 1999).
- ⁸ Daleo J. A., Ellison K. A., Boone D. H., "Metallurgical Considerations for Life Assessment and the Safe Refurbishment and Re-qualification of Gas Turbine Blades" (Paper presented at the ASME/IGTI TURBO EXPO 2000, Munich, Germany May 8-11, 2000).
- ⁹ K. A. Ellison and J. A. Daleo, "Microstructural Evaluation of MCrAlY / Superalloy Interdiffusion Zones" (Paper presented at the IOM conference "Life Assessment of Hot Section Gas Turbine Components", James Watt Centre, Heriot Watt University, Edinburgh, UK, Oct. 5 7 1999), 31.
- ¹⁰ J. S. Kirkaldy and L. C. Brown, "Diffusion Behaviour in Ternary, Multiphase Systems", <u>Canadian Metallurgical Quarterly</u>, 2 (1963), 89 - 115.

- ¹¹ A. Taylor and R. W. Floyd, "The Constitution of Nickel-Rich Alloys of the Nickel-Chromium-Aluminum System", <u>J. Inst.</u> Met., 81 (1952-1953), 451-464.
- ¹² S. M. Merchant and M. R. Notis, "A Review: Constitution of the Al-Cr-Ni System", <u>Materials Science and Engineering</u>, 66 (1984), 47-60.
- ¹³ C. C. Jia, K. Ishida and T. Nishizawa, "Partition of Alloying Elements Between (A1), '(L1₂) and (B2) Phases in Ni-Al Base Systems", <u>Metallurgical and Materials Transactions A</u>, 25A (1994), 473 485.
- ¹⁴ C. T. Sims, "Prediction of Phase Composition", in <u>Superalloys</u> <u>II</u>, ed. C.T. Sims, N.S. Stoloff, and W.C. Hagel (New York: John Wiley & Sons, 1987), 217-240.
- ¹⁵ W. D. Manly and P. A. Beck (NACA Technical Note 2602, February 1952).
- ¹⁶ B. G. Livshits and N. N. Myuller, "Investigations of the Phase Equilibria in the Co-Cr-Al System" (in Russian), <u>Nauch. Doklady</u> <u>Vyssh. Shkoly</u>, 3 (1958), 201-206.
- ¹⁷ B. G. Livshits and N. N. Myuller, "Phase Equilibria in the Co-Cr-Al System" (in Russian), <u>Sbornik Moscov. Inst. Stali</u>, 39 (1960), 267-283.
- ¹⁸ J. Schramm, "Das Dreistoffsystem Nickel-Kobalt-Aluminium", Zeitschrift für Metallkunde, 33 (1941), 403-412.